TWO-PHASE PIV FOR PARTICLE-LADEN FLOWS

Chunhui Pan
Department of Mechanical Engineering
University of Maryland
College Park, MD 20742

Ken Kiger
Department of Mechanical Engineering
University of Maryland
College Park, MD 20742

ABSTRACT

The present study has developed a specialized Particle Image Velocimetry (PIV) image processing technique which can be applied to solid-liquid two-phase turbulent flows. The main principle of the technique is to utilize a 2-D median filter to separate images of the two phases, thus eliminating the errors induced by the distinct motion of the dispersed component. The main influence of the median filter on the accuracy of the displacement calculation is due to the filter width f. This has been studied in the present research by using 6 groups of different sized dispersed particles ranging from $d_p = 45$ μm to 300 μm in combination with tracer particles with an effective image size of $d_t \sim 15$ μm. The results have shown that the errors introduced by the filter are negligible, and mainly arise from the regions of large velocity gradients which are sensitive to the slight loss of information incurred by the processing. The filter width f also affects the algorithm's ability to correctly separate and identify the dispersed phase particles from the two-phase images. The number of correctly identified dispersed phase particles was found to increase with the particle size, and decrease with the filter width. Above a critical size $d_p/d_t \approx 5.0$, the particle size had no significant influence on the number of particles identified, or the accuracy of the displacement calculation. The results also indicated that the optimal filter width required to balance the separation of phases and the accuracy of calculation was $f/d_t \approx 2.5$.

1. INTRODUCTION

Particle-laden turbulent flows cover a wide range of applications from pollution control and sediment transport, to combustion processes and erosion effects in gas turbines. In the last two decades, many improvements have been made in measurement technology to advance the knowledge of physical mechanisms and dynamics of such flows. The most commonly used measurement techniques, such as Laser Doppler Anemometry and Phase Doppler Anemometry, are single point measurements which provide useful statistical information of fluid velocity, particle velocity, particle size and concentration. One limitation of single-point measurements, however, is the difficulty associated with interpreting the data into meaningful physical mechanisms which control the dynamics between the phases. Thus to reach a good understanding of multi-phase flows, the microscale information of the inter-phase dynamics and its structure relative to the carrier fluid is essential.

In contrast to single point measurements, PIV represents an instantaneous whole field technique which makes it possible to detect spatial flow structure and provide a direct indication of the inter-phase coupling. One of the critical requirements of PIV measurement is to calculate the displacements of tracer particles by means of cross-correlation or autocorrelation performed within an interrogation volume. For multi-phase flows, however, the presence of the discrete particles will affect the PIV evaluation. Figure 1 shows a sample two-phase image of a particle-laden channel flow seeded with hollow silver-coated glass beads as PIV tracer particles (diameter, $d_t = 15$ μm), and transparent glass beads as discrete particles (diameter, $d_p = 300$ μm). The velocity field computed by standard PIV techniques without any specialized treatment is illustrated in Figure 2. Spurious vectors occur in the vicinity of the discrete particles, due to the fact that there are significant differences between the motion of particles and carrier fluid. In order to utilize PIV in the measurement of multiphase flows, standard PIV processing techniques need to be modified to eliminate the interference effects caused by the disparate motions of each phase.

In surveying recent literature, several examples can be found where PIV has been applied to the simultaneous measurement of both phases. For example, Sato, et al. (1995) used two CCD cameras with optical filters combined with multivolume illumination to accurately detect discrete phase particulates relative to tracer particles in a water channel flow. However, due to the correlation influence between the phases as noted above, no carrier phase vectors could be detected

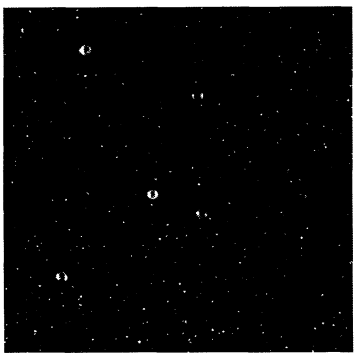

Figure 1. Sample of a two-phase images.

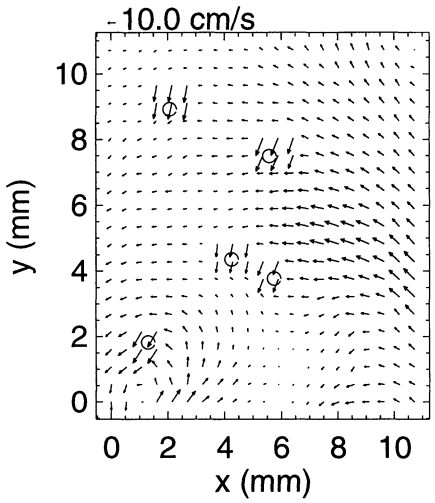

Figure 2. Vector field of carrier phase using standard PIV. Circles represent locations of dispersed phase particles. Note the influence of the particles on the velocity field.

near the location of the discrete particles. Fluorescent particles (Fujiwara, 1998) have also been used to separate discrete and tracer particle information in two-phase bubbly flow. This technique, however, requires the use of two synchronized cameras and a powerful laser to produce adequate fluorescent images. Finally, bulk motion methods based on discriminating separate correlation peaks representing the discrete motion of both the dispersed phase and carrier fluid are being developed (Westerweel, 1997). This technique promises to be useful for high concentration flows of very fine particles but, because the method is based upon the bulk average motion of the dispersed phase, the details of the interaction terms may not be clear. The motivation for the present study, then is to provide a reliable, single-camera technique that could resolve the local particle/fluid interaction within the flow. To accomplish this goal, an image processing technique has been

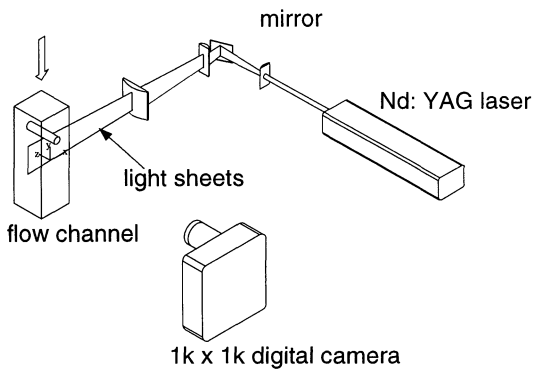

Figure 3. The sketch of experiment setup.

Particle type	diameter (μm)	image diameter (pixels)	d_p/d_t
PIV tracer, d_t	15	2	1
discrete, d_p	53-45	3-4	1.5-2
discrete, d_p	90-75	6-8	3-4
discrete, d_p	106-90	8-10	4-5
discrete, d_p	125-106	10-12	5-6
discrete, d_p	212-180	13-15	6.5-7.5
discrete, d_p	300	20	10

Table 1. Properties of particles used in the present study

developed to eliminate the dispersed phase influence for dilute solid-liquid flows, and applied to several experimental test cases. The technique is based on the existence of image pattern differences between the PIV tracer particles and the discrete (dispersed) phase particles, and utilizes a 2-D median filter to separate the two phases.

2. EXPERIMENTAL SETUP

The experimental test cases for the technique have all examined heavy particle sedimentation in the turbulent wake of a cylinder. A vertical, recirculating water channel (Figure 3) with a 100 mm by 100 mm square cross-section and a maximum velocity of 100 mm/s were used to conduct the tests. The images were acquired 25 mm downstream of a 12 mm diameter cylinder, at a Reynolds number of 840 based on the cylinder diameter. The test section was illuminated by a high speed pulsed Nd:YAG laser ($\lambda = 532nm$) with a pulse intensity of 15 mJ. The image area was approximately 24 mm $\times$ 24 mm, and recorded using a Kodak Megaplus ES1.0 camera with a 200 mm lens ($f\# = 8$) and a time separation of 3 ms between image pairs. Hollow silver-coated glass spheres with average diameter of 15 μm, and a specific gravity around 1.5 were seeded as PIV tracer particles in the flow. Six groups of different size transparent glass spheres with diameters ranging from 45 μm to 300 μm were used as discrete particles. The properties of the particles are listed in table 1.

3. THE IMAGE PROCESSING TECHNIQUE OF PHASE SEPARATION

To eliminate the effect of two co-existent phases, a two-dimensional median filter is employed to separate the larger dispersed phase particle image from the carrier phase tracer particle image. The carrier phase is then obtained by subtracting the filtered image from the original two-phase image. In order to reduce the errors introduced by the separation process, the filter width must be selected to balance separation efficiency and accuracy.

3.1 The principle of phase separation

A median filter is a nonlinear signal processing technique, that has been found effective in reducing random noise and periodic interference patterns without severely degrading the signal (Huang, 1981). In PIV image processing, the property of preserving sharp edges makes the filter useful because it allows more information about the original image to be maintained. This is especially important in regions of high shear, where the ratio of signal to noise is relatively low. For a two-phase image with both small tracer particles and big discrete particles, the small tracer particles can be regarded as noise scattered over a uniform background. To remove the small tracer particles, a median filter is performed by convolving a square two-dimensional filter window A, of width $N \times N$ pixels, over all the pixels within the image. For each position (i_o, j_o) of the window A, the filter sorts the gray level values of region A into ascending order and then selects the median value to replace pixel (i_o, j_o). This is stated mathematically by equation (1):

$$X^1_{i,j} < \ldots < X^k_{i,j} \ldots < X^N_{i,j} \quad (i,j) \in A \tag{1}$$

$$Y_{i_o,j_o} = X^k_{i,j} \tag{2}$$

where Y_{i_o,j_o} is the filtered value, $X_{i,j}$ is an element of the input image, and the superscript k represents the median value of the region. This implies the effect of the median filter is to reduce the variance, and increase the ratio of signal to noise in the image. The median value computed at one window position is independent of the value computed at another window position.

Provided the filter window size is small enough, the gray level values of the pixels (i.e. image background) are nearly homogeneous inside the window. Only a small portion of pixels (at the location of the tracer particles) in the window would be "noise" pixels, which will generally have gray level values in the extreme rank position, and hence will be removed. When the filter window moves over a discrete particle, the image intensity is dominated by the pattern of the discrete particle, and the median value will reflect a value close to the original. Thus after filtering, the small tracer particles are removed, leaving only the discrete particles. The filter width is a critical parameter to determine whether the two phases are separated properly.

3.2 Evaluation of the discrete particles

After filtering, only discrete particles remain on the image, and their motion is calculated using a correlation tracking method as shown in Figure 4. First, a reference particle

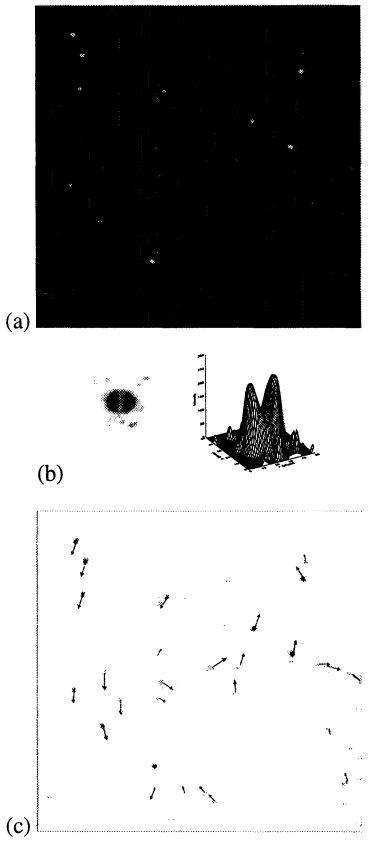

Figure 4. (a) Dispersed phase (filtered) image. (b) Image and surface of reference particle. (c) The corresponding velocity field.

is selected as a template and convoluted with the whole image to identify discrete particles (Figure 4b). Since the discrete particles have a form similar to the reference particle, the peaks in the convolution correspond to center locations of the individual dispersed particles. (see Figure 4c). A peak-finding algorithm is then used to identify discrete particles, and a cross-correlation tracking method is performed to calculate the displacements between the discrete particle image pairs.

3.3 Evaluation of the tracer particles

Once the displacement field of the dispersed phase has been obtained, the motion of the carrier phase can be determined. This is accomplished using an extraction technique which obtains a single-phase image of tracer particles, $S_{i,j}$, from the original two-phase image, $T_{i,j}$, by subtraction:

$$S_{i,j} = T_{i,j} - median(T_{i,j}) \quad (i,j) \in Z^2 \tag{3}$$

where $median(T_{i,j})$ is the two-dimensional median filtered output of the original image, and Z is the domain of the image.

An example of the carrier phase image of tracer particles, $S_{i,j}$, is shown in Figure 5(a). The velocity field of the carrier

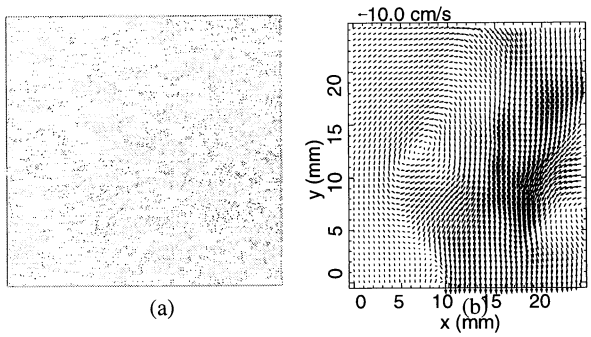

Figure 5. a) Carrier phase image is created by subtracting filtered image from the original. b) Standard PIV technique applied to carrier phase image to obtain the corresponding velocity field.

phase shown in Figure 5(b) is calculated through a standard cross-correlation method applied to the tracer particle images.

3.4 The validation of the technique

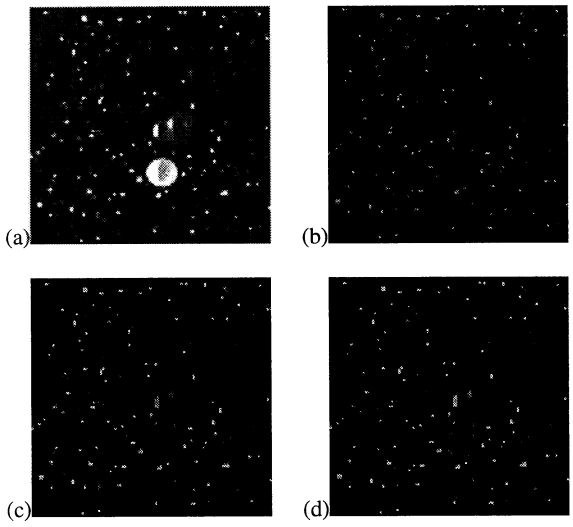

Figure 6. (a) Two-phase image. (b) Carrier phase image obtained with the filter width = 3.0. (c) Carrier phase image obtained with the filter width = 5.0. (d) Carrier phase image obtained with the filter width = 7.0. d_p = 300μm, d_t = 10μm.

The median filter width will affect the information of both phases extracted from a two-phase image. In turn, this may influence the accurate calculation of the displacement through residual "artifacts" left by the image separation process. Figure 6 illustrates how the information content within a carrier phase image changes with the filter width. For small filter width, the discrete particle is completely removed, whereas for increasing filter width, a residual image around the periphery of the discrete particle remains. This results from an erosion of the particle by the larger filter, and hence an incomplete removal when it is subtracted from the original image. These slight changes may induce errors in the displacement calculation of both phases. The goal of the present work is to quantify these effects and assess the optimal filter parameters to ensure accurate calculations.

In order to achieve these goals, the phase separation technique has been tested by using a series of artificial two-phase images composed of two separate single phase images; one which contains only PIV tracer particles, the other which contains only discrete particles. The results of the composition process are illustrated in Figure 7, which is obtained from equation:

$$T_{i,j} = 255 < ((P_{i,j} - N_{noise}) > 0 + S_{i,j}) > 0, \qquad (4)$$

where N_{noise} is the average background noise of the dispersed phase, and $P_{i,j}$ is the image of the dispersed phase particles. The velocity field of the carrier phase is then calculated in two ways: 1) by applying standard PIV technique to the original single phase image, and 2) by applying the separation technique to the artificial two-phase image and recalculating the tracer particle displacements (see Figure 8). The errors induced by the median filter are investigated by computing the absolute and relative variance between the two displacement fields in the direction of streamwise and spanwise coordinates of the fluid motion. Filter widths of 3, 5, and 7 pixels are tested for 6 different groups of discrete particle size. The average error is then calculated using

$$x_{err} = \frac{1}{MN} \sum_{i=1}^{i=N} \sum_{j=1}^{j=M} |\Delta x_{(i,j),\triangle_f} - \Delta x_{(i,j),orig}| \qquad (5)$$

$$x_{err}/x_0 = \frac{1}{MN} \sum_{i=1}^{i=N} \sum_{j=1}^{j=M} \left| \frac{\Delta x_{err(i,j),\triangle_f} - \Delta x_{(i,j),orig}}{U_{(i,j),orig}} \right| \qquad (6)$$

where $M \times N$ is the number of carrier fluid vectors in each image. The total error is then calculated for 10 independent image pairs for each case. This represents 23000 velocity measurements for the carrier fluid and approximately 1200 to 1800 measurements for the particles depending on their size. The results are shown in Figure 9, 10, and 11.

4. DISCUSSION

The accuracy of displacements for both phases calculated from the separated images is influenced by the median filter width and the discrete particle size. In the following, Section 4.1 discusses the effect of these parameters on the tracer particle motion, followed by a similar discussion for the discrete particles in Section 4.2.

4.1 The influence of median filter width on the velocity fields

The effect of the filter width and discrete particle size on the calculation of the tracer particle displacement is shown for a specific example in Figure 8, and the average error results are shown in Figure 9. The main conclusion to be drawn from these results is that the filtering process produces a negligible

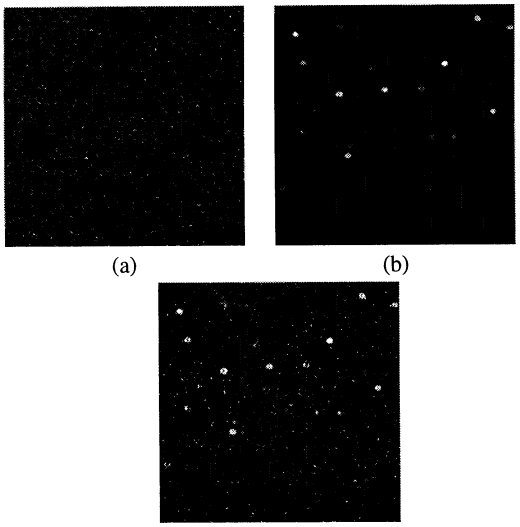

Figure 7. (a) Discrete particles extracted from a real two-phase image. (b) A real tracer phase image. (c) The artificial image reconstructed by adding (a) to (b)

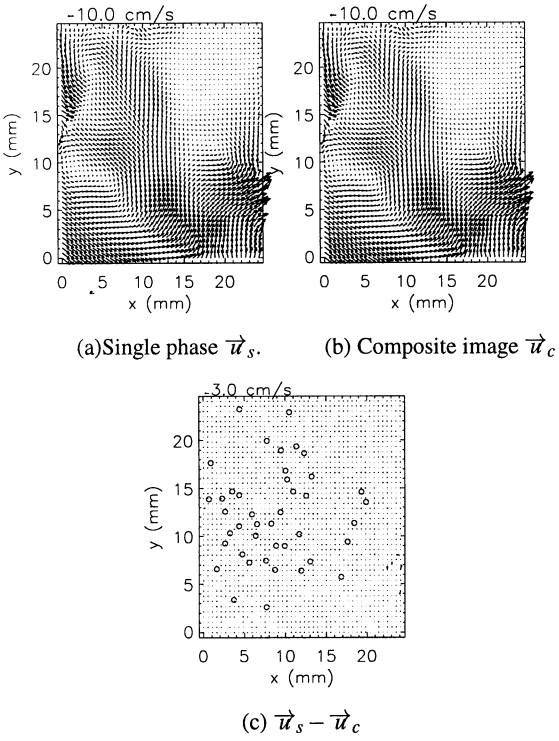

(a)Single phase $\vec{u}_s$. (b) Composite image $\vec{u}_c$

(c) $\vec{u}_s - \vec{u}_c$

Figure 8. The errors induced by a median filter with filter width = 5.

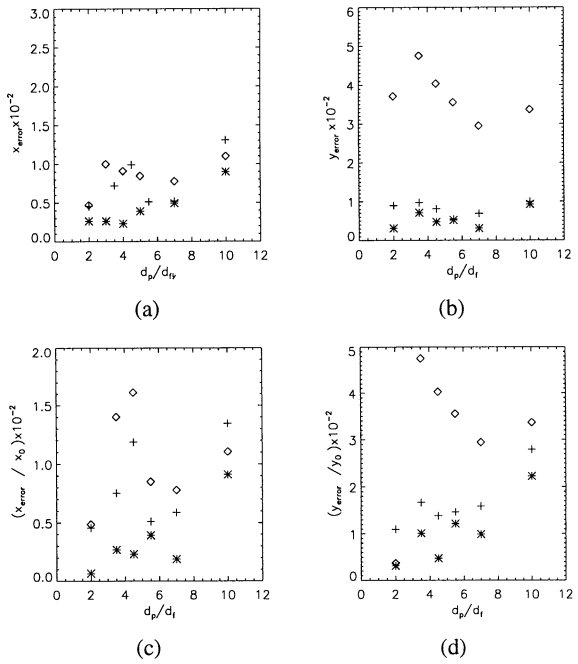

Figure 9. Absolute and relative displacement variance of carrier phase. (a) absolute streamwise. (b) absolute spanwise. (c) relative streamwise. (d) relative spanwise. +, filter width = 3; ∗, filter width = 5; ◇, filter width = 7.

error in the carrier phase displacement. From the average results in Figure 9, it is observed that the absolute value of the error is less than 0.01 pixels for the optimal filter. Normalized with respect to the actual displacement, this corresponds to an error of around 1% for the flow speeds and timings used in the current experiment. It can also be seen that the errors are very small for the majority of the flow map (Figure 8c), and sizable errors only occur in limited regions not associated with a discrete particle. Upon further examination, these regions are more closely correlated to areas of large gradients. High shear regions typically have low signal to noise ratios which produce poorly resolved correlation peaks. When the filtering process is applied, it removes a small amount of correlation information, and hence makes the area more susceptible to errors.

The optimum filter width for the separation process is observed to consistently be a 5 pixel window, which corresponds to a nondimensional size of $f/d_t \approx 2.5$. Filter widths smaller than this value decrease the correlation peak through the removal of some of the larger tracer particles, while larger filter sizes leave residual "artifacts" of the discrete particles as shown in Figure 8. In general, there is also a slight increase in the error as the size of the discrete particles is increased. This may be due to the increased area of the "voids" left in the single phase image after the discrete particles are removed, which decreases the number of tracer particles available to construct the proper correlation near the boundary of the particles.

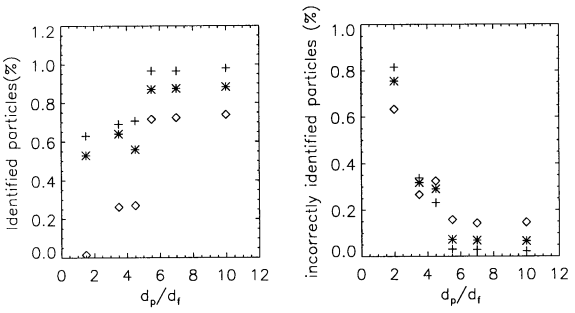

Figure 10. (a) The correctly identified number of particles versus the different size of particles. (b) Incorrectly identified particles versus the different size of particles. +, filter width = 3; ∗, filter width = 5; ◇, filter width = 7.

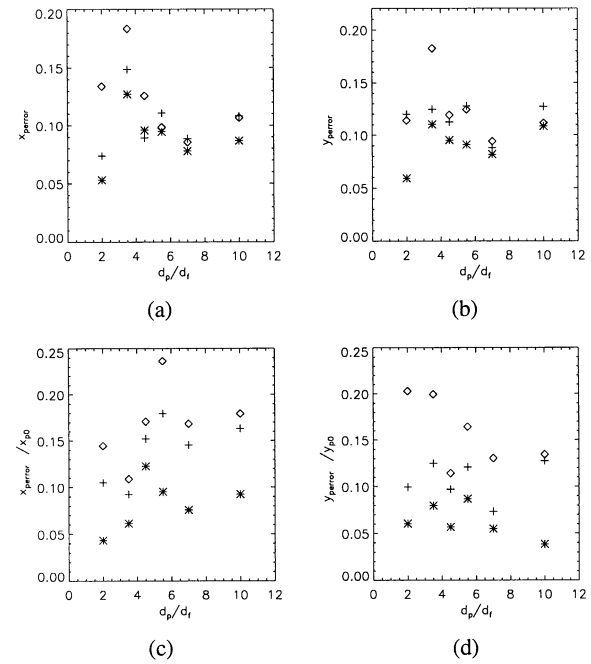

Figure 11. Absolute and relative displacement variance of dispersed phase. a) absolute streamwise. b) absolute spanwise. c) relative streamwise d) relative spanwise. +, filter width = 3; ∗, filter width = 5; ◇, filter width = 7.

4.2 The influence of filter and particle size on discrete phase displacement

The effect of filter width and discrete particle size on the accurate identification of the discrete particles is shown in Figure 10. The results indicate that the smaller filter widths do a better job of separating the phases, and that above a critical discrete particle size of $d_p/d_t > 5$, little change is observed in the number of particles correctly identified. This is consistent with the fact that the image size of the dispersed phase particles will vary depending on whether they happen to be in the center of the light sheet or near the dimmer edge of the sheet. The greater the separation in size between the filter and the particles (large d_p/d_t, small f/d_t), then a greater number of the discrete particles will be retained by the separation process.

The effect of the filter width on the displacement of the discrete particles is shown in Figure 11. The error for these displacements is about an order of magnitude larger than those for the tracer particle calculation. Thus the average absolute error is about 0.1 pixel, and the relative error is on the order of 10% (note that the relative error will depend on the timing and flow conditions of the experiment). Considering that the typical uncertainty of a subpixel interpolation estimate is on the order of 0.1 pixel, this does not represent a major increase in the particle's calculated displacement. The optimal filter width is again the intermediate value of $f/d_t \approx 2.5$, but there is no strong trend with the various discrete particle sizes.

5. CONCLUSIONS

The above discussion indicates that the median filter width should be selected to optimize the minimum error incurred on both the carrier phase displacement and to maximize the correct identification of the dispersed phase particles. The optimal value is given by a filter width of $f/d_c > 2$, and discrete phase particles should then be larger than $d_p/d_c > 4$. These conditions give average displacement errors in the tracer flow field of on the order of 0.01 pixels, but the errors are primarily caused by a small number of vectors which are modified in the region of large shear. The displacement errors of the dispersed phase particles will be larger, and are typically on the order of 0.1 pixels. These conditions will also ensure that almost 90% of the dispersed phase particles are correctly identified.

6 ACKNOWLEDGEMENTS

The authors would like to thank the National Science Foundation for their generous support of this work under grant numbers CTS9702723 and CTS9871156.

REFERENCES

uang, T. S., 1981 *Two-dimentional digital signal processing II.* Springer-Verlag, Berlin.

ato, Y., Hanzawa, A., Hishida, K., and Maeda, M., 1995, "Interactions between Particle wake and turbulence in a water channel flow(PIV measurements and modeling for turbulence modification)", *Advances in Multiphase Flow* 1995. Elsevier Science B.V.

ujiwara, A., Tokuhiro, A., Hishida, K., and Maeda, M., 1998, " Investigation of oscillatiory bubble motion using a dual shadow technique and its surrounding flow field by LIF-PIV". *Third international conference on multiphase flow, ICMF'98*, Lyon, France, June 8-12.

esterweel, J., Delnoij, E., and Ytsma, M., 1997, "Measurement of two-phase flow using ensemble-correlation PIV," *50th annual meeting of the American Physical Society Division of Fluid Dynamics*, San Francisco, Nov. 23-25.